METABOLISM

Nicotinamide mononucleotide increases muscle insulin sensitivity in prediabetic women

Mihoko Yoshino[1]†, Jun Yoshino[1]†, Brandon D. Kayser[1], Gary J. Patti[2], Michael P. Franczyk[1], Kathryn F. Mills[3], Miriam Sindelar[2], Terri Pietka[1], Bruce W. Patterson[1], Shin-Ichiro Imai[3], Samuel Klein[1]*

In rodents, obesity and aging impair nicotinamide adenine dinucleotide (NAD^+) biosynthesis, which contributes to metabolic dysfunction. Nicotinamide mononucleotide (NMN) availability is a rate-limiting factor in mammalian NAD^+ biosynthesis. We conducted a 10-week, randomized, placebo-controlled, double-blind trial to evaluate the effect of NMN supplementation on metabolic function in postmenopausal women with prediabetes who were overweight or obese. Insulin-stimulated glucose disposal, assessed by using the hyperinsulinemic-euglycemic clamp, and skeletal muscle insulin signaling [phosphorylation of protein kinase AKT and mechanistic target of rapamycin (mTOR)] increased after NMN supplementation but did not change after placebo treatment. NMN supplementation up-regulated the expression of platelet-derived growth factor receptor β and other genes related to muscle remodeling. These results demonstrate that NMN increases muscle insulin sensitivity, insulin signaling, and remodeling in women with prediabetes who are overweight or obese (clinicaltrial.gov NCT 03151239).

Nicotinamide adenine dinucleotide (NAD^+) is a cosubstrate for NAD^+-consuming enzymes that are essential in the regulation of diverse biological processes. In rodents, inadequate NAD^+ biosynthesis in liver, adipose tissue, and skeletal muscle contributes to the pathogenesis of obesity- and aging-associated metabolic abnormalities, including insulin resistance, β cell dysfunction, and hepatic steatosis (*1*–*9*). The primary pathway for NAD^+ biosynthesis involves the conversion of nicotinamide to nicotinamide mononucleotide (NMN) and subsequent conversion of NMN to NAD^+ (*5*). The production of NMN is the key rate-limiting factor in mammalian NAD^+ biosynthesis. Systemic NMN administration in obese mice fed a high-fat diet increases tissue NAD^+ concentrations and improves glucose tolerance, insulin sensitivity, and β cell function (*1*, *4*, *10*), and long-term NMN administration in mice fed regular chow mitigates age-associated insulin resistance (*11*). The beneficial effects of NMN supplementation in rodents has led to rapid commercial development of NMN products for people, and NMN is marketed in the United States and other countries as a supplement that improves glucose control, enhances energy metabolism, and reverses the metabolic complications of aging. Although NMN is present in natural foods—including edamame, broccoli, avocado, tomatoes, and milk—the daily amount of NMN that is normally consumed as part of a healthy diet is likely less than 2 mg/day (*5*). The dose of NMN available in commercial products ranges from 50 to 150 mg per capsule, and some consumers take two 150-mg capsules daily. However, we are not aware of studies on the metabolic effects of daily NMN supplementation in people.

We conducted a 10-week, randomized, placebo-controlled, double-blind trial in postmenopausal women with prediabetes who were overweight or obese (body mass index of 25.3 to 39.1 kg/m^2) to determine the effects of NMN supplementation on (i) body composition, (ii) skeletal muscle insulin sensitivity and insulin signaling; and (iii) muscle NAD^+ content and global gene expression profile. We specifically studied postmenopausal women because NMN treatment caused greater beneficial metabolic effects in female mice than in male mice with diet-induced diabetes (*1*).

Twenty-five postmenopausal women with prediabetes based on criteria proposed by the American Diabetes Association (*12*) who were overweight or obese completed this study; 12 were randomized to the placebo group and 13 to the NMN group (250 mg/day; Oriental Yeast Co., Ltd., Tokyo, Japan) (fig. S1). Baseline testing included (i) dual-energy x-ray absorptiometry and magnetic resonance imaging to assess body composition; (ii) a hyperinsulinemic-euglycemic clamp procedure (4-hour basal stage and 4-hour insulin infusion at 50 mU/m^2/min), in conjunction with stable isotope glucose and palmitate tracer infusions to assess multiorgan insulin sensitivity; and (iii) percutaneous biopsies of quadriceps muscle during the basal period and insulin infusion to assess cellular effects of NMN treatment. After baseline studies were completed, participants were randomly assigned to 10 weeks of treatment with placebo or NMN. After participants completed ~10 weeks of treatment, all study procedures conducted at baseline were repeated. In addition, peripheral blood mononuclear cell (PBMC) NAD^+ content was assessed for 4 hours after placebo or NMN ingestion. On the basis of weekly pill counts, 99.6% of prescribed pills in the placebo group and 100% of prescribed pills in the NMN group were taken by the participants. No adverse events were reported, and no abnormalities in standard blood tests were detected in either group (table S1).

Plasma concentrations of *N*-methyl-2-pyridone-5-carboxamide and *N*-methyl-4-pyridone-5-carboxamide, which are metabolites produced by NMN (*13*), increased after 10 weeks of NMN, but not placebo, treatment (Fig. 1A). Basal NAD^+ content in PBMCs increased after 10 weeks of NMN treatment but did not change after placebo treatment (Fig. 1B). Ingestion of a single 250-mg dose of NMN at the end of 10 weeks of treatment did not cause a further increase above the basal value in PBMC NAD^+ content, as assessed in serial blood samples obtained for 240 min after ingestion (Fig. 1C); however, the 240-min PBMC NAD^+ content area under the curve (AUC) above zero was 43% greater ($P < 0.01$) in the NMN group than in the placebo group because of the higher basal value in the NMN group (Fig. 1D). Quadriceps muscle tissue samples were obtained 1.5 hours after the last dose of placebo or NMN to assess the effect of treatment on skeletal muscle NMN metabolites. Although muscle NAD^+ and nicotinamide content did not change after 10 weeks of treatment in either group (Fig. 1, E and F), muscle *N*-methyl-nicotinamide, methyl-2-pyridone-5-carboxamide, and *N*-methyl-4-pyridone-5-carboxamide increased after NMN, but not placebo, treatment (Fig. 1, G to I), suggesting that NMN treatment increased muscle NAD^+ turnover.

Body composition (fat mass, fat-free mass, intra-abdominal adipose tissue volume, and intrahepatic triglyceride content), blood pressure, plasma glucose, insulin, free fatty acid, lipid, adiponectin and leptin concentrations, and both basal glucose and fatty acid kinetics did not change in either group after 10 weeks of treatment (Table 1). When compared with pretreatment values, muscle insulin sensitivity, assessed as the rate of insulin-stimulated glucose disposal per kilogram of fat-free mass during the clamp procedure, was 25 ± 7% greater after 10 weeks of NMN supplementation ($P < 0.01$) but was not different after placebo treatment (Fig. 2A). By contrast, hepatic insulin sensitivity [assessed as the hepatic insulin sensitivity index (*14*) and the suppression of glucose rate of appearance (Ra) during insulin infusion] and adipose tissue insulin sensitivity [assessed as the adipose tissue insulin resistance index (*15*) and the suppression of palmitate Ra] were not different after treatment with either placebo or NMN (fig. S2) when compared with pretreatment values.

We evaluated the effect of NMN supplementation on phosphorylation of serine-473 and threonine-308 of the protein kinase AKT

[1]Center for Human Nutrition, Washington University School of Medicine, St. Louis, MO, USA. [2]Department of Chemistry, Washington University School of Medicine, St. Louis, MO, USA. [3]Department of Developmental Biology, Washington University School of Medicine, St. Louis, MO, USA.
*Corresponding author. Email: sklein@wustl.edu
†These authors contributed equally to this work.

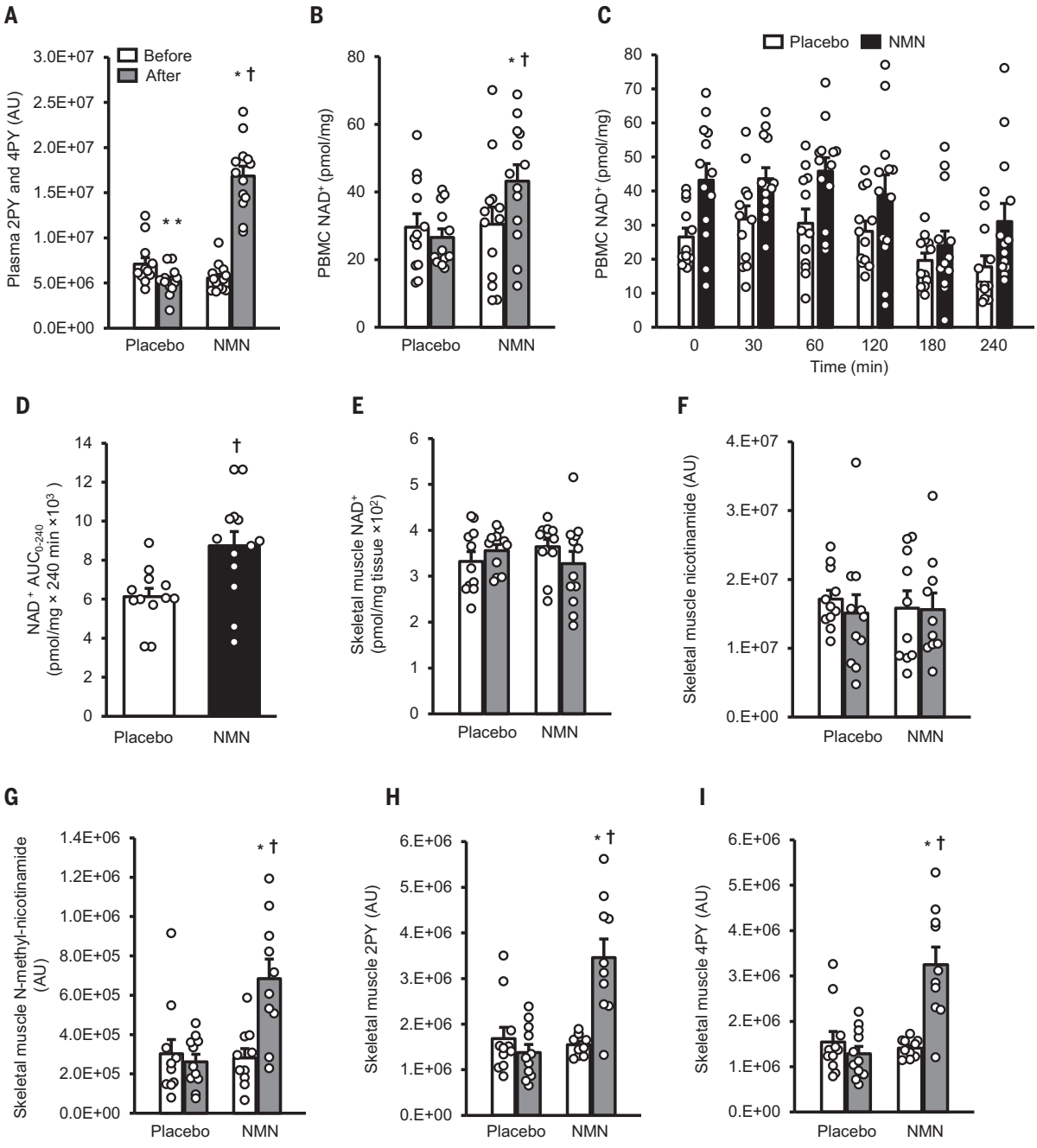

Fig. 1. NMN metabolites and NAD$^+$ in plasma, PBMCs, and skeletal muscle. (**A**) Plasma *N*-methyl-2-pyridone-5-carboxamide (2PY) and *N*-methyl-4-pyridone-5-carboxamide (4PY) before (white bars) and after (gray bars) treatment. AU, arbitrary units. (**B**) Basal PBMC NAD$^+$ content before (white bars) and after (gray bars) treatment. (**C**) PBMC NAD$^+$ content before (time 0) and for 240 min after ingesting a placebo capsule (white bars) or NMN (250 mg) (black bars) at the end of 10 weeks of treatment with placebo or NMN. (**D**) PBMC NAD$^+$ AUC for 240 min after ingesting a placebo capsule or 250 mg of NMN. (**E** to **I**) Skeletal muscle NAD$^+$ (E), nicotinamide (F), *N*-methyl-nicotinamide (G), 2PY (H), and 4PY (I) contents before (white bars) and after placebo or NMN treatment (gray bars). Two-way mixed model analysis of variance (ANOVA) with time (before versus after treatment) and group (placebo versus NMN) as factors was used to compare the effect of treatment with NMN and placebo on basal PBMC and tissue NAD$^+$. A significant time-by-group interaction is followed by Tukey's post hoc test to locate significant mean differences. A Student's *t* test for independent samples (two-tailed) was used to determine differences between the mean PBMC AUC values in the two groups. *Value significantly different from corresponding before-treatment value, $P < 0.01$. **Value significantly different from corresponding before-treatment value, $P < 0.05$. †Value significantly different from corresponding value in the placebo group, $P < 0.01$. Circles represent individual participant values: Skeletal muscle NAD$^+$ content was measured in 11 placebo and 12 NMN participants, skeletal muscle NMN metabolites were measured in 11 placebo and 10 NMN participants, and all other measurements are from 12 placebo and 13 NMN participants. Error bars represent means ± SEM.

Table 1. Body composition and basal metabolic variables. Values are means ± SEM. Metabolic variables were measured before and after placebo (n = 12) or NMN (n = 13) treatment. A two-way mixed model ANOVA was used to evaluate the effect of NMN supplementation on each outcome. The effect of NMN on these variables was not different from placebo. FFM indicates fat-free mass.

Variables	Placebo		NMN		Repeated measures ANOVA		
	Before	After	Before	After	P_{group}	P_{time}	$P_{group\ x\ time}$
Age (years)	61 ± 5	No change	62 ± 4	No change	Not determined	Not determined	Not determined
Body weight (kg)	87 ± 3	87 ± 3	89 ± 4	89 ± 4	0.764	0.917	0.941
Body mass index (kg/m^2)	33.4 ± 1.0	33.3 ± 0.9	33.7 ± 1.4	33.8 ± 1.5	0.928	0.917	0.941
Fat mass (kg)	40.3 ± 2.0	39.9 ± 2.0	42.8 ± 2.9	42.9 ± 3.0	0.547	0.672	0.702
Fat-free mass (kg)	45.6 ± 0.9	46.1 ± 0.7	44.8 ± 1.2	45.5 ± 1.3	0.654	0.011	0.846
Intrahepatic triglyceride content (%)	14.8 ± 2.0	15.7 ± 2.5	6.3 ± 1.2	6.8 ± 1.3	0.003	0.385	0.461
Intra-abdominal adipose tissue volume (cm^3)	1576 ± 71	1669 ± 95	1492 ± 213	1504 ± 214	0.265	0.180	0.186
Systolic blood pressure (mmHg)	128 ± 4	131 ± 4	126 ± 5	125 ± 5	0.089	0.813	0.686
Diastolic blood pressure (mmHg)	73 ± 3	77 ± 3	73 ± 3	75 ± 3	0.832	0.286	0.701
Hemoglobin A1C (%)	5.5 ± 0.1	5.5 ± 0.1	5.7 ± 0.1	5.5 ± 0.1	0.407	0.008	0.396
Glucose (mmol/liter)	5.7 ± 0.2	5.6 ± 0.2	5.7 ± 0.1	5.6 ± 0.2	0.906	0.379	0.836
Insulin (μU/ml)	16.7 ± 2.0	17.2 ± 2.5	13.6 ± 1.9	15.8 ± 2.7	0.400	0.122	0.335
Free fatty acids (g/liter)	0.198 ± 0.018	0.183 ± 0.011	0.192 ± 0.014	0.193 ± 0.015	0.973	0.493	0.492
Triglyceride (mmol/liter)	1.63 ± 0.22	1.48 ± 0.23	1.39 ± 0.25	1.26 ± 0.18	0.289	0.107	0.554
High-density lipoprotein cholesterol (mmol/liter)	1.28 ± 0.07	1.34 ± 0.07	1.25 ± 0.10	1.30 ± 0.10	0.804	0.071	0.930
High–molecular weight adiponectin (μg/ml)	4.02 ± 0.53	3.93 ± 0.51	3.90 ± 0.49	3.86 ± 0.52	0.900	0.564	0.843
Leptin (ng/ml)	83.5 ± 8.1	82.4 ± 6.8	88.1 ± 6.7	88.5 ± 7.3	0.589	0.916	0.811
Basal glucose Ra (μmol/kg FFM/min)	15.5 ± 0.4	15.4 ± 0.4	15.7 ± 0.4	16.1 ± 0.5	0.469	0.459	0.311
Basal palmitate Ra (μmol/kg FFM/min)	2.66 ± 0.29	2.23 ± 0.17	2.28 ± 0.21	2.21 ± 0.18	0.455	0.098	0.247

and phosphorylation of serine-2448 of mechanistic target of rapamycin (mTOR) in muscle, which are key components of the insulin signaling pathway involved in regulating glucose uptake and muscle remodeling. Muscle AKT and mTOR phosphorylation and total AKT and mTOR protein abundance during insulin infusion were greater after than before treatment in the NMN group but did not change in the placebo group (Fig. 2, B and C, and fig. S3). These cellular findings are consistent with the effects of placebo and NMN treatment on muscle insulin sensitivity observed in vivo.

We used RNA sequencing (RNA-seq) to evaluate global gene expression of quadriceps muscle samples. We identified differentially expressed genes [DEGs; false discovery rate (FDR) <0.05] after versus before 10 weeks of placebo or NMN treatment during basal conditions and insulin infusion (Fig. 3A and table S2). During the basal conditions, there were 21 DEGs in the placebo group and 15 DEGs in the NMN group after treatment compared with before treatment (Fig. 3A and table S2). During insulin infusion, there were 5 DEGs in the placebo group and 308 DEGs in the NMN group after treatment compared with before treatment; none of the DEGs in the NMN group were affected by placebo treatment (Fig. 3A and table S2).

Database for Annotation, Visualization and Integrated Discovery pathway analysis was used to identify the gene ontology (GO) terms that were significantly enriched (adjusted P value <0.05) with the 308 DEGs during insulin infusion after NMN treatment. The "platelet-derived growth factor (PDGF) binding" pathway was the most highly enriched (Fig. 3B and table S3). DEGs were significantly enriched in biological pathways of collagen and extracellular matrix metabolism, which are downstream elements of PDGF signaling (Fig. 3B and table S3). Moreover, NMN supplementation significantly up-regulated skeletal muscle expression of PDGF receptor β (*PDGFR*β) and markers of skeletal muscle pericytes (*CD90* and *CD109*) during insulin infusion (Fig. 3C). Supplementation with NMN also increased the expression of other genes related to myogenic PW1-positive interstitial cells and pericytes (PW1/PEG3, QPRT, NG2, and PECAM1) (*16*, *17*), but these increases did not achieve statistical significance (fig. S4). In addition, the expression of downstream targets of PDGF signaling—such as *COL1A1*, *COL5A1*, and *COL6A1*—was significantly up-regulated after NMN treatment (Fig. 3C). These results indicate that NMN treatment increased myogenic cell populations and enhanced PDGF signaling in skeletal muscle.

Because of the importance of NAD^+ biology on mitochondrial function and the relationship between muscle mitochondria and muscle function (*3*, *18*), we evaluated whether NMN affected skeletal muscle mitochondrial respiratory capacity and physical function. Muscle mitochondrial oxidative capacity, assessed by using high-resolution respirometry of quadriceps muscle samples obtained by percutaneous biopsy, did not change after 10 weeks of treatment with either placebo or NMN (fig. S5). Muscle physical function—assessed by measuring handgrip strength and torque, fatigability, and recovery from fatiguing exercise of knee extensors and flexors of the dominant leg—were not affected by 10 weeks of placebo or NMN treatment (fig. S6).

This randomized, placebo-controlled, double-blind trial demonstrates that 10 weeks of NMN supplementation increases muscle insulin signaling (increased insulin-stimulated phosphorylated AKT and mTOR) and muscle insulin sensitivity (increased insulin-stimulated glucose disposal rate expressed per kilogram of fat-free mass) in postmenopausal women with prediabetes who are overweight or obese. This improvement in muscle insulin sensitivity is clinically relevant and similar to the improvement observed after ~10% weight loss (*19*) and after 12 weeks of treatment with the insulin-sensitizing agent troglitazone (*20*) in people with obesity. The increases in muscle insulin-stimulated AKT phosphorylation and glucose uptake after NMN treatment that were observed in our participants are consistent with studies conducted in rodent models (*1*, *3*, *11*). Our data suggest that an NMN-induced increase in muscle *PDGFR*β expression could be involved in mediating this effect, because PDGF signaling, particularly through PDGFRβ, enhances insulin-stimulated AKT phosphorylation and

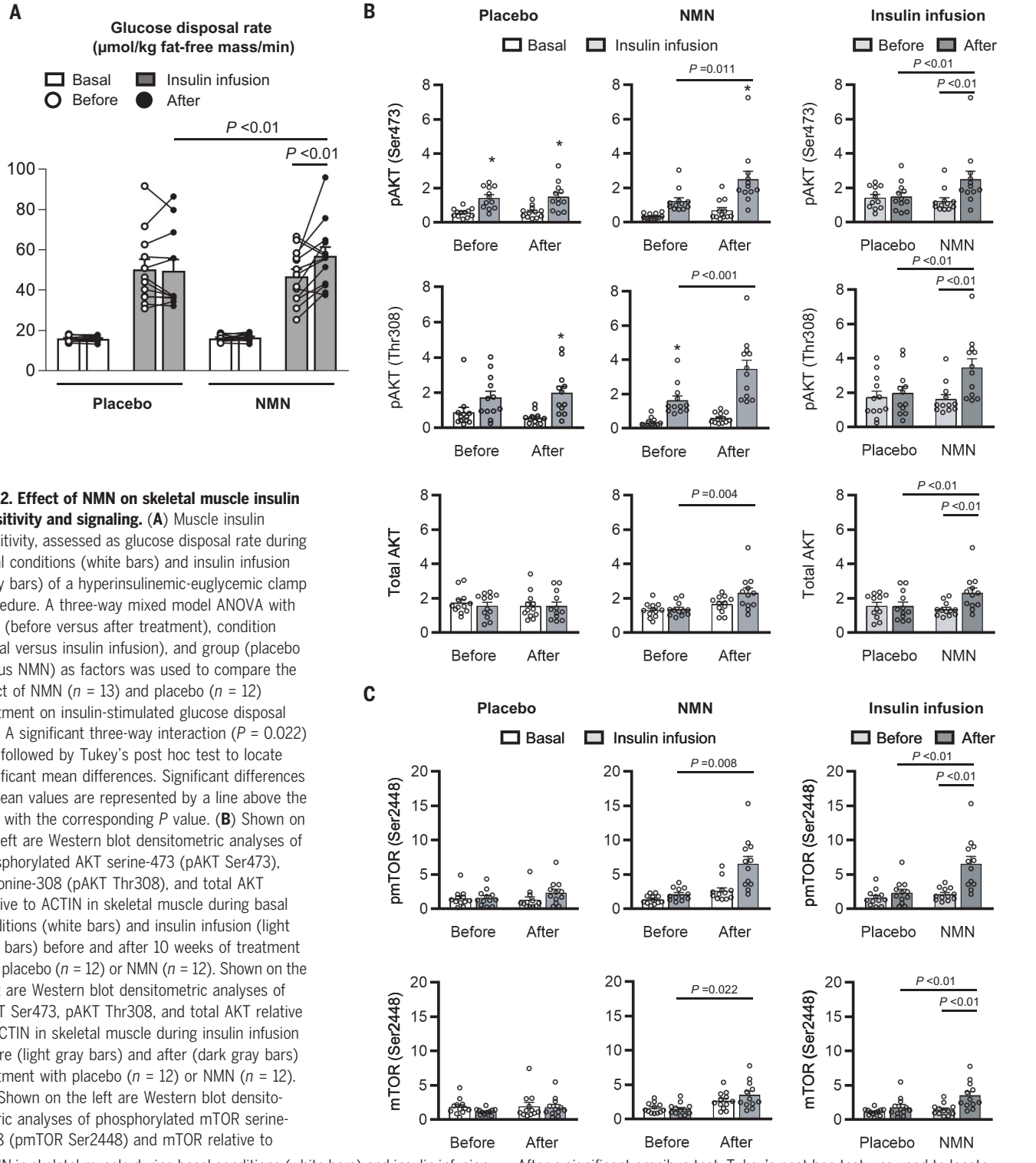

Fig. 2. Effect of NMN on skeletal muscle insulin sensitivity and signaling. (**A**) Muscle insulin sensitivity, assessed as glucose disposal rate during basal conditions (white bars) and insulin infusion (gray bars) of a hyperinsulinemic-euglycemic clamp procedure. A three-way mixed model ANOVA with time (before versus after treatment), condition (basal versus insulin infusion), and group (placebo versus NMN) as factors was used to compare the effect of NMN (n = 13) and placebo (n = 12) treatment on insulin-stimulated glucose disposal rate. A significant three-way interaction (P = 0.022) was followed by Tukey's post hoc test to locate significant mean differences. Significant differences in mean values are represented by a line above the bars with the corresponding P value. (**B**) Shown on the left are Western blot densitometric analyses of phosphorylated AKT serine-473 (pAKT Ser473), threonine-308 (pAKT Thr308), and total AKT relative to ACTIN in skeletal muscle during basal conditions (white bars) and insulin infusion (light gray bars) before and after 10 weeks of treatment with placebo (n = 12) or NMN (n = 12). Shown on the right are Western blot densitometric analyses of pAKT Ser473, pAKT Thr308, and total AKT relative to ACTIN in skeletal muscle during insulin infusion before (light gray bars) and after (dark gray bars) treatment with placebo (n = 12) or NMN (n = 12). (**C**) Shown on the left are Western blot densitometric analyses of phosphorylated mTOR serine-2448 (pmTOR Ser2448) and mTOR relative to ACTIN in skeletal muscle during basal conditions (white bars) and insulin infusion (light gray bars) before and after placebo (n = 12) or NMN (n = 12). Shown on the right are Western blot densitometric analyses of pmTOR Ser2448 and mTOR relative to ACTIN in skeletal muscle during insulin infusion before (light gray bars) and after (dark gray bars) placebo (n = 12) or NMN (n = 12) treatment. Raw images for individual Western blot analyses are provided in the supplementary materials (fig. S3). One-way ANOVA was performed to determine differences in the quantity of phosphorylated AKTs among each combination of time and condition (during basal and insulin infusion before and after each treatment) within each group. After a significant omnibus test, Tukey's post hoc test was used to locate significant mean differences. Two-way mixed model ANOVA with time (before versus after treatment) and group (placebo versus NMN) as factors was used to determine the significance of differences between variables during insulin infusion. A significant two-way interaction was followed by Tukey's post hoc test to locate significant mean differences. Significant differences in mean values are represented by a line above the bars with the corresponding P value. *Value significantly different from the corresponding basal value, $P < 0.05$. Circles represent individual participant values. Error bars represent means ± SEM.

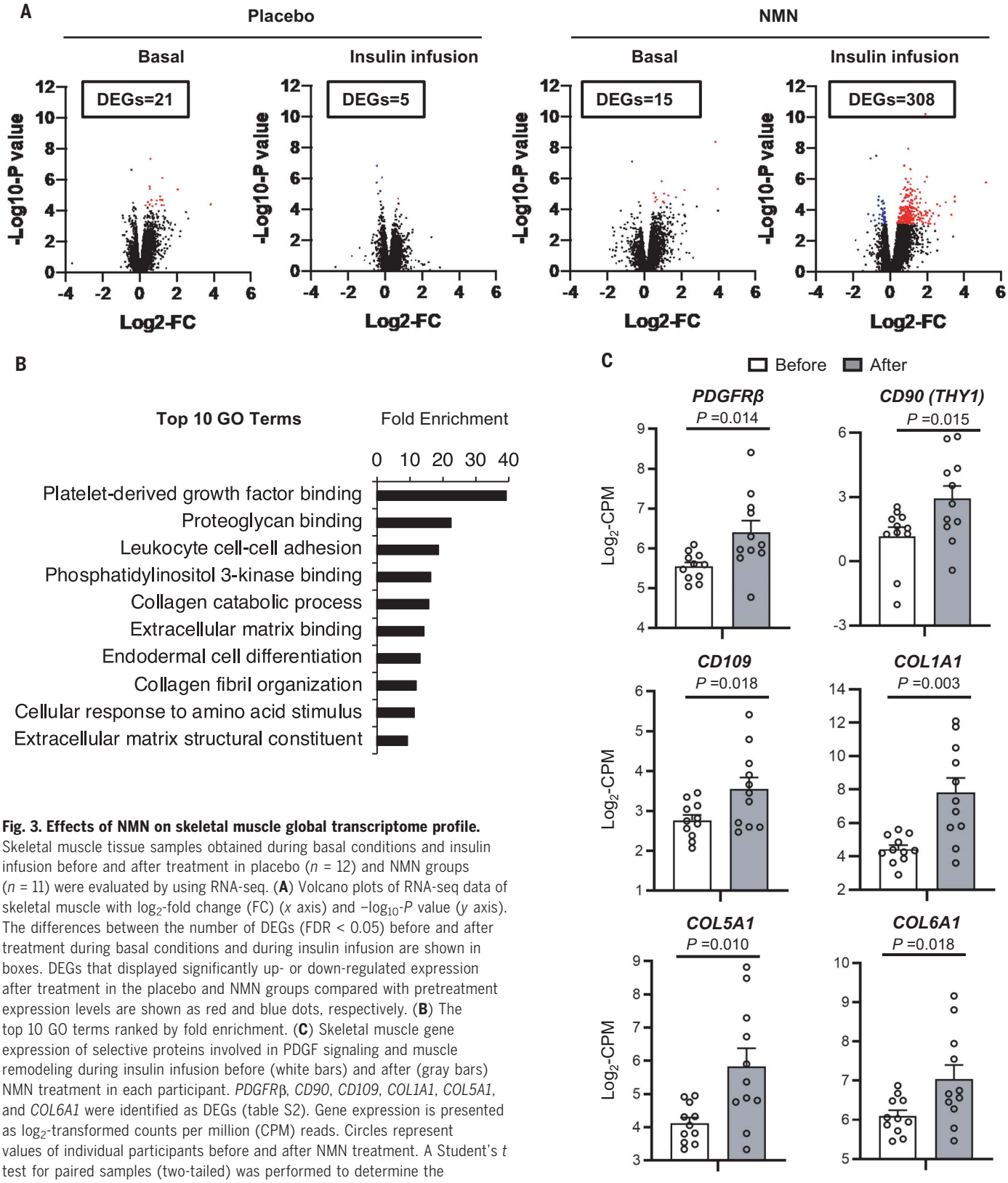

Fig. 3. Effects of NMN on skeletal muscle global transcriptome profile. Skeletal muscle tissue samples obtained during basal conditions and insulin infusion before and after treatment in placebo (n = 12) and NMN groups (n = 11) were evaluated by using RNA-seq. (**A**) Volcano plots of RNA-seq data of skeletal muscle with $\log_2$-fold change (FC) (x axis) and $-\log_{10}$-P value (y axis). The differences between the number of DEGs (FDR < 0.05) before and after treatment during basal conditions and during insulin infusion are shown in boxes. DEGs that displayed significantly up- or down-regulated expression after treatment in the placebo and NMN groups compared with pretreatment expression levels are shown as red and blue dots, respectively. (**B**) The top 10 GO terms ranked by fold enrichment. (**C**) Skeletal muscle gene expression of selective proteins involved in PDGF signaling and muscle remodeling during insulin infusion before (white bars) and after (gray bars) NMN treatment in each participant. *PDGFRβ*, *CD90*, *CD109*, *COL1A1*, *COL5A1*, and *COL6A1* were identified as DEGs (table S2). Gene expression is presented as $\log_2$-transformed counts per million (CPM) reads. Circles represent values of individual participants before and after NMN treatment. A Student's t test for paired samples (two-tailed) was performed to determine the difference between expression levels before and after NMN treatment for each gene; corresponding P values are indicated above the black lines. Error bars represent means ± SEM.

glucose transport in skeletal muscle and multiple cell types (*21*–*23*). The absence of changes in steady-state levels of muscle NAD^+ in our NMN-treated participants is also consistent with studies conducted in mice that found that NMN administration improved insulin sensitivity without changing muscle NAD^+ concentration (*11*). However, NMN treatment increased the levels of muscle NMN metabolites (*N*-methyl nicotinamide, *N*-methyl-2-pyridone-5-carboxamide, and *N*-methyl-4-pyridone-5-carboxamide), suggesting that NMN treatment increased skeletal muscle NAD^+ turnover. The effect of NMN was specific to insulin sensitivity in muscle and did not affect other important variables associated with insulin resistance, including indices of liver and adipose tissue insulin sensitivity, intra-abdominal adipose tissue volume, intrahepatic triglyceride content, and fasting plasma glucose, insulin, and adiponectin concentrations. These results demonstrate that NMN has selective beneficial effects on insulin-mediated glucose metabolism in skeletal muscle.

Our data demonstrate a robust effect of NMN on skeletal muscle biology. The data obtained from our unbiased global transcriptome profiling of skeletal muscle demonstrate that compared with placebo, NMN caused a 60-fold increase in the number of DEGs during insulin infusion. The PDGF binding pathway was the most highly enriched with DEGs, and expression of muscle *PDGFR*β and downstream targets of PDGF signaling was significantly up-regulated during insulin infusion after NMN treatment. In addition, NMN treatment increased insulin-stimulated mTOR phosphorylation and gene expression of selected markers of myogenic PW1/PEG3-positive interstitial cells and pericytes (*16*, *17*), which together indicate increased skeletal muscle remodeling and regeneration.

In contrast to the insulin-sensitizing effects of NMN that we observed in our participants, the results from several randomized controlled trials conducted in middle-aged and older adult men found that treatment with nicotinamide riboside (NR), another NAD^+ intermediate that improves insulin sensitivity in rodents (*5*, *8*, *24*), did not affect whole-body or muscle insulin sensitivity (*25*–*27*). The reason for the absence of metabolic benefits of NR supplementation in these clinical studies is not known, and further studies are needed to address this issue.

The results from our study demonstrate that NMN supplementation (250 mg/day) increases skeletal muscle insulin signaling, insulin sensitivity, and muscle remodeling in postmenopausal women with prediabetes who are overweight or obese. The precise mechanism or mechanisms responsible for these metabolic effects and the potential metabolic benefits of NMN supplementation in other patient populations remain to be explored.

REFERENCES AND NOTES

1. J. Yoshino, K. F. Mills, M. J. Yoon, S. Imai, *Cell Metab.* **14**, 528–536 (2011).
2. K. M. Ramsey, K. F. Mills, A. Satoh, S. Imai, *Aging Cell* **7**, 78–88 (2008).
3. A. P. Gomes *et al.*, *Cell* **155**, 1624–1638 (2013).
4. K. L. Stromsdorfer *et al.*, *Cell Rep.* **16**, 1851–1860 (2016).
5. J. Yoshino, J. A. Baur, S. Imai, *Cell Metab.* **27**, 513–528 (2018).
6. S. Imai, J. Yoshino, *Diabetes Obes. Metab.* **15**, 26–33 (2013).
7. E. Verdin, *Science* **350**, 1208–1213 (2015).
8. E. Katsyuba, M. Romani, D. Hofer, J. Auwerx, *Nat Metab* **2**, 9–31 (2020).
9. M. R. McReynolds, K. Chellappa, J. A. Baur, *Exp. Gerontol.* **134**, 110888 (2020).
10. G. M. Uddin, N. A. Youngson, D. A. Sinclair, M. J. Morris, *Front. Pharmacol.* **7**, 258 (2016).
11. K. F. Mills *et al.*, *Cell Metab.* **24**, 795–806 (2016).
12. American Diabetes Association, *Diabetes Care* **43**, S14–S31 (2020).
13. J. Irie *et al.*, *Endocr. J.* **67**, 153–160 (2020).
14. G. I. Smith *et al.*, *J. Clin. Invest.* **130**, 1453–1460 (2020).
15. E. Fabbrini *et al.*, *J. Lipid Res.* **53**, 321–324 (2012).
16. A. Pannérec, L. Formicola, V. Besson, G. Marazzi, D. A. Sassoon, *Development* **140**, 2879–2891 (2013).
17. M. Crisan *et al.*, *Cell Stem Cell* **3**, 301–313 (2008).
18. D. W. Frederick *et al.*, *Cell Metab.* **24**, 269–282 (2016).
19. F. Magkos *et al.*, *Cell Metab.* **23**, 591–601 (2016).
20. J. J. Nolan, B. Ludvik, P. Beerdsen, M. Joyce, J. Olefsky, *N. Engl. J. Med.* **331**, 1188–1193 (1994).
21. M. Razmara, C. H. Heldin, J. Lennartsson, *Cell Commun. Signal.* **11**, 3 (2013).
22. B. H. Rauch, A. Weber, M. Braun, N. Zimmermann, K. Schrör, *FEBS Lett.* **481**, 3–7 (2000).
23. K. L. Hoehn *et al.*, *Cell Metab.* **7**, 421–433 (2008).
24. C. Cantó *et al.*, *Cell Metab.* **15**, 838–847 (2012).
25. O. L. Dollerup *et al.*, *Am. J. Clin. Nutr.* **108**, 343–353 (2018).
26. Y. S. Elhassan *et al.*, *Cell Rep.* **28**, 1717–1728.e6 (2019).
27. C. M. E. Remie *et al.*, *Am. J. Clin. Nutr.* **112**, 413–426 (2020).

ACKNOWLEDGMENTS

We thank J. Shew, F. Custodio, A. Okunade, S. Johnson, K. Tokizane, and H. C. Lei for their laboratory technical assistance; S. Torbitzky, Z. Boger, M. Giuffrida, J. Britt, and the Clinical and Translational Research Unit staff for their assistance in conducting the studies; the study subjects for their participation; and Oriental Yeast Co., Ltd. (Tokyo, Japan) for providing placebo and NMN capsules. **Funding:** This study was supported by NIH grants DK56341, DK104995, AG037457, and AG047902; the UC San Diego IGM Genomics Center, which has an Illumina NovaSeq 6000 that was purchased with funding from a NIH SIG grant (#S10 OD026929); the Tanaka Fund; and the Foundation for Barnes-Jewish Hospital. **Author contributions:** M.Y. and B.D.K. conducted the clinical studies. J.Y., M.P.F., K.F.M., B.W.P., G.J.P., M.S., and T.P. performed the sample analyses. M.Y., J.Y., G.J.P., B.W.P., S.I., and S.K. analyzed and interpreted the data. M.Y., J.Y., S.I., and S.K. wrote the manuscript. S.K. designed and supervised the studies and obtained funding for the work. S.K. is the guarantor of this work and, as such, had full access to all the data in the study and takes responsibility for the integrity of the data and the accuracy of the data analysis. All authors critically reviewed and edited the manuscript. **Competing interests:** S.I. receives a part of patent-licensing fees from MetroBiotech (USA) and Teijin Limited (Japan) through Washington University. S.I. also serves as Invited Chief Scientist at the Institute for Biomedical Research and Innovation in Kobe, Japan, which does not involve competing interests. J.Y. is listed as an inventor on a US patent application related to NMN (no. 20180228824). S.K. receives research support from Janssen Pharmaceuticals and serves on a scientific advisory board for Merck Sharp & Dohme Corp. The other authors have nothing to disclose. **Data and materials availability:** All data in this paper are presented in the main text and supplementary materials. This study is registered at clinicaltrials.gov (https://clinicaltrials.gov/) as no. NCT03151239. The skeletal muscle sequencing datasets generated during the current study are available in the Gene Expression Omnibus (GEO) database (www.ncbi.nlm.nih.gov/geo) under accession no. GSE157988.

SUPPLEMENTARY MATERIALS

science.sciencemag.org/content/372/6547/1224/suppl/DC1
Materials and Methods
Figs. S1 to S6
Tables S1 to S4
References (*28*–*34*)
MDAR Reproducibility Checklist
Data S1

View/request a protocol for this paper from *Bio-protocol*.

27 September 2020; accepted 8 April 2021
Published online 22 April 2021
10.1126/science.abe9985

Science

Nicotinamide mononucleotide increases muscle insulin sensitivity in prediabetic women

Mihoko Yoshino, Jun Yoshino, Brandon D. Kayser, Gary J. Patti, Michael P. Franczyk, Kathryn F. Mills, Miriam Sindelar, Terri Pietka, Bruce W. Patterson, Shin-Ichiro Imai and Samuel Klein

Science **372** (6547), 1224-1229.
DOI: 10.1126/science.abe9985originally published online April 22, 2021

Anti-aging supplement effects in humans

Synthesis of nicotinamide adenine dinucleotide (NAD^+) decreases during aging, which is thought to limit the activity of enzymes that require it for their catalytic activity. Studies in animals indicate that replenishment of cellular NAD^+ can have beneficial effects on aging and age-related diseases, but the situation in humans is less clear. Yoshino *et al.* report the effects of supplementation with the NAD^+ precursor nicotinamide mononucleotide in overweight or obese postmenopausal women with prediabetes (see the Perspective by Hepler and Bass). The treatment improved insulin sensitivity in muscle, although a change in NAD^+ content was not detected. The treatment also increased the expression of platelet-derived growth factor b. The results support potential therapeutic action of NAD^+ supplementation in humans, but how various NAD+ precursors are processed in specific tissues remains to be fully explored.

Science, abe9985, this issue p. 1224; see also abj0764, p. 1147